[CANCER RESEARCH 63, 282–286, January 15, 2003]

Advances in Brief

Increased Nuclear Phosphatase and Tensin Homologue Deleted on Chromosome 10 Is Associated with G_0-G_1 in MCF-7 Cells[1]

Margaret E. Ginn-Pease and Charis Eng[2]

Clinical Cancer Genetics Program [C. E.] and Human Cancer Genetics Program [M. E. G-P., C. E.], Comprehensive Cancer Center, Columbus, Ohio 43210; Division of Human Genetics [C. E.], Department of Internal Medicine, Division of Human Cancer Genetics [M. E. G-P., C. E.], Department of Molecular Virology, Immunology and Medical Genetics, and Department of Molecular Genetics [C. E.], The Ohio State University, Columbus, Ohio 43210; and Cancer Research UK Human Cancer Genetics Research Group, University of Cambridge, Cambridge CB2 2XZ, United Kingdom [C. E.]

Abstract

Phosphatase and tensin homologue deleted on chromosome 10 (PTEN) is a tumor suppressor that causes cell cycle arrest. Lack of a nuclear locator sequence and a function in the cytosolic phosphatidylinositol 3′-kinase/Akt pathway diverted its study from the nucleus. However, immunohistochemistry revealed PTEN in the nucleus of normal cells and decreased nuclear PTEN in neoplastic tissues. Using protein expression analysis and fluoroscopic localization of green fluorescence protein-tagged PTEN, we examined nuclear PTEN in MCF-7 cells. We demonstrate that PTEN enters the nucleus and that nuclear PTEN varies throughout the cell cycle. Higher nuclear PTEN levels were associated with G_0-G_1 phase, and lower nuclear PTEN levels were associated with S phase. We postulate that nuclear PTEN activity might directly regulate the cell cycle.

Introduction

The 9-exon *PTEN*[3] encodes a 403-residue tumor suppressor protein with several structural and functional motifs including homology to tensin (aa 5–182), a catalytic phosphatase domain (aa 122–133), two proline-glutamate-serine-threonine degradation sequences, and a postsynaptic density protein/*Drosophila* disc large/zona occludens-1-binding domain (aa 400–403; Refs.1 and 2). Only aa 10–353 are necessary for cell cycle effects, Akt inhibition, and protein and lipid phosphatase functions (3). Although many structural features have been identified, and their function has been characterized, no NLS has been described. Therefore, reported nuclear PTEN studies have been limited to immunohistochemical studies in breast, thyroid, and endocrine pancreatic tumors; cutaneous melanoma; esophageal squamous cell carcinoma; and colorectal carcinoma compared with normal counterpart tissue (4–8). In these studies, a shift from nuclear to cytoplasmic PTEN correlated with increasing neoplasia for all tissues. Nuclear PTEN has also been noted in a study of mouse neurodevelopment (9) and in anecdotal observations by researchers describing differential localization with a non-naturally occurring Δ354–403 and a serine/threonine mutant (3), all of which could be artifactual. The discovery of a PTEN-like dual-specificity phosphatase, CDC14, in the nucleus (10) further led researchers to partition PTEN function to the cytoplasm, subsequently describing CDC14 function with p53 in the nucleus and the role of PTEN with p53 in the cytoplasm. Although PTEN has been shown by several research groups to have effects on the cell cycle and its component proteins by arresting cells in G_1 (11–13), the role of PTEN in cell cycle control may extend beyond the suppression exerted on the phosphatidylinositol 3′-kinase/Akt pathway and beyond its characterized mechanism in the cytosol. The nuclear-cytoplasmic movement of a phosphatase is not without precedent. Another phosphatase, CDC25B, has been shown to shuttle between the cytosol and the nucleus during the cell cycle in HeLa cells (14), with localization controlled by nuclear export/import sequences. Because PTEN has been observed in the nucleus and has cell cycle effects, we hypothesize that PTEN shuttling may be associated with the cell cycle. In this study, we sought to directly demonstrate PTEN in the nucleus of MCF-7 breast cancer cells through both biochemical and direct visualization methods and, furthermore, to correlate nuclear PTEN levels with the cell cycle.

Materials and Methods

Cell Lines. The MCF-7 Tet-off cell line (BD Clontech, Inc.), a breast cancer cell line containing a Tet-controlled cassette, was grown in DMEM supplemented with 10% fetal bovine serum, 1% penicillin-streptomycin, and 100 μg/ml Geneticin (G418; all supplied by Life Technologies, Inc.). Hygromycin B (200–400 μg/ml; Invitrogen, Inc.) was used to select stable clones incorporating the experimental pTre2Hyg constructs. Vector expression was controlled with Tet (1–2 μg/ml).

Plasmid Construction and Transfection. *PTEN* cDNA was cut out from a vector described previously (12) and inserted into the Tet-controlled pTre2Hyg vector (BD Clontech, Inc.). *PTEN* cDNA was also cloned into the pEGFPC1 vector (BD Clontech, Inc.) downstream of EGFPC1. EGFPC1-PTEN-WT was cut and subcloned into the pTre2Hyg vector. Fidelity of the constructs was confirmed by sequencing. The pTre2Hyg, pTre2Hyg PTEN-WT, and pTre2Hyg EGFPC1-PTEN-WT vectors were stably transfected into the MCF-7 Tet-off cell line (Fugene; Roche Applied Biosciences) using procedures recommended by the manufacturer.

Cell Cycle Experiments. Tet was removed by washing twice with Tet-free medium, once with PBS (Invitrogen, Inc.), and replating in Tet-free or Tet-supplemented medium; medium was replaced after 24 h. After 48 h without Tet, medium was augmented with HU (3 mM) for 16–18 h to synchronize the cells. Cells were released from HU by replacement of medium. After removal from HU, samples were harvested from culture at time points (mainly 0, 4, 6, 7, 8, 9, 10, 12, 15, and 24 h) to allow the cells to complete one cell cycle (21–24 h). Cells remained under Tet-supplemented medium for several time points as controls. At harvest, cells were 70–90% confluent.

Western Blot Analysis and Protein Detection. After medium removal, the MCF-7 cells were washed and scraped into PBS. The cells were divided for cell cycle analysis and for nuclear/cytoplasmic protein separation. Nuclear and cytoplasmic proteins were isolated with a buffer extraction system and centrifugation according to the manufacturer's recommendations (NE-Per; Pierce Biotechnology, Inc., Rockford, IL). The extraction buffers follow a classical method of low to high salt for nuclear and cytoplasmic separation. To the cytoplasmic extraction the following inhibitors were added: 0.75 mM phenyl-

Received 10/11/02; accepted 11/27/02.

The costs of publication of this article were defrayed in part by the payment of page charges. This article must therefore be hereby marked *advertisement* in accordance with 18 U.S.C. Section 1734 solely to indicate this fact.

[1] Supported in part by American Cancer Society Grant RSG-02-151-01-CCE (to C. E.), Susan G. Komen Breast Cancer Research Foundation Grant BCTR 2000 462 (to C. E.), and National Cancer Institute Grants T32CA09338 (to M. E. G-P.) and P30CA16058 (to the Comprehensive Cancer Center). C. E. is a recipient of Doris Duke Distinguished Clinical Science Award.

[2] To whom requests for reprints should be addressed, at Division of Human Genetics, Department of Internal Medicine and Human Cancer Genetics Program, The Ohio State University, 420 West 12th Avenue, Suite 690 TMRF, Columbus, OH 43210. Phone: (614) 292-2347; Fax: (614) 688-3582; E-mail: eng-1@medctr.osu.edu.

[3] The abbreviations used are: PTEN, phosphatase and tensin homologue, deleted on chromosome 10; aa, amino acid(s); NLS, nuclear locator sequence; Tet, tetracycline; EGFP, enhanced green fluorescence protein; WT, wild type; HU, hydroxyurea; LDH, lactate dehydrogenase; MVP, major vault protein; RB, retinoblastoma.

methylsulfonyl fluoride; 0.5 mg/ml bezamidine hydrochloride; 2 μg/ml each of leupeptin, aprotinin, and pepstatin; 10 mM β-glycerophosphate; 0.2 mM sodium orthovanadate; and 25 mM sodium fluoride. The nuclear extract solution was supplemented with 2 mM phenylmethylsulfonyl fluoride and the above inhibitors listed for the cytoplasmic extracts. Protein concentrations were determined using the bicinchoninic assay reagents and the microbicinchoninic assay method (Pierce Biotechnology, Inc.). Although cross-contamination of samples using the above Pierce reagents is low, nuclear proteins were verified using an alternate method of nuclear protein extraction, Western blot with antibodies against RB (BD Biosciences) and E2F family proteins (Santa Cruz Biotechnology, Santa Cruz, CA) and LDH activity. Cells were subjected to sucrose preps using 0.33 M, 0.88 M, and 1 M discontinuous sucrose gradients in HEPES buffer with proteinase inhibitors with centrifugation. Protein concentrations were determined using a Bradford assay (Bio-Rad protein assay; Bio-Rad Corp.). Nuclear extracts were subjected to Western blotting as described below. Cytoplasmic contamination was further examined by determining the LDH activity of cytoplasmic and nuclear extracts. A standard protocol with NADH and pyruvate substrates was used, and activity was measured as decreasing absorbance at 340 nm on a spectrophotometer (SpectraMax; Molecular Diagnostics). For Western blot analysis, 10 or 20 μg of protein were fractionated by 10% SDS-polyacrylamide gels, transferred to nitrocellulose membrane (Bio-Rad Corp.), and probed using a primary monoclonal antibody to PTEN (6H2.1; 1:1000) and a secondary antimouse horseradish peroxidase antibody (Promega, Madison, WI; 1:5000). The proteins were detected using enhanced chemiluminescence (ECL reagents; Amersham Pharmacia Corp., Piscataway, NJ) and blots exposed to film [XAR (Kodak); Hyperfilm (Amersham Pharmacia Corp.)]. Equal loading of lanes was evaluated by staining membranes with Ponceau S reagent (Sigma Chemical Co.).

Cell Cycle Analysis. At time course points for nuclear and cytoplasmic extraction, the divided cells were centrifuged, resuspended in cold 70% ethanol, and stored at –20°C until analysis. Washed cells were stained in 0.1% Triton X-100 in PBS with 1 μg/ml propidium iodide (Sigma Chemical Co.). Flow cytometry was performed using a Beckman-Coulter elite flow cytometer using a 610 long pass filter for data collection. Data were filtered, and cell cycle phases were quantified using the Modfit program (Verity Software, Bowdoin, ME).

Microscopy. Cells were grown on well slides (Labtek, Inc.) in tandem with cells for nuclear-cytoplasmic extracts and cell cycle analysis and similarly treated with Tet and HU. At harvest, cells were washed with PBS, fixed with 0.5–4% paraformaldehyde (depending on subsequent staining procedures), and stored at 4°C. Before slide imaging, slides were stained with Hoechst 33342 (Sigma Chemical Co.) to visualize nuclei. Cells were viewed with a Nikon ECLIPSE E800 fluorescence microscope fitted with filters for EGFP and Hoechst 33342 identification and equipped with a computer-supported imaging system (SpotCAM; Diagnostic Instruments, Inc.). Background correction settings with the computer support were standardized for all slides in a given time course series. Images were processed using the Adobe Photoshop program. At least seven fields of each slide were examined to note nuclear and cytoplasmic cellular EGFPC1-PTEN-WT. To further confirm nuclear entry of EGFPC1-PTEN-WT, the nucleus was also identified by staining cells with a monoclonal antibody to CDK2 (Santa Cruz Biotechnology), a noncycling nuclear protein, and, subsequently, an antimouse rhodamine secondary antibody (Pierce Biotechnology, Inc.). Cells were viewed and imaged using the system described above and a rhodamine filter.

Results and Discussion

To determine whether PTEN can exist in the nucleus and whether nuclear-cytoplasmic localization is related to the cell cycle, the MCF-7 Tet-off breast cancer cell line was stably transfected with PTEN-WT (pTre2Hyg PTEN-WT), EGFPC1-PTEN-WT (pTre2Hyg EGFPC1-PTEN-WT), and empty vector (pTre2Hyg). MCF-7 was chosen because we have carefully characterized this model with respect to PTEN and changes in other cell cycle components after transfection of PTEN-WT and naturally occurring PTEN mutants associated with neoplasia (12). Furthermore, MCF-7 has wild type PTEN, p53, and RB. The cells were examined for the presence of nuclear and cytoplasmic PTEN by Western blot analysis using a monoclonal antibody against the COOH-terminal 100 aa of PTEN (6H2.1; Fig. 1). Nuclear PTEN and cytoplasmic PTEN were observed in all three clones. Of note, overexpression of PTEN or EGFPC1-PTEN resulted in increased PTEN protein levels in both the cytosol and nucleus. To further confirm the presence of PTEN in the nuclear extracts, an alternative method of nuclear isolation was used. Nuclei were isolated from cells from all three cell lines by a sucrose gradient fractionation technique (see "Materials and Methods") and subjected to Western blotting with 6H2.1. Endogenous PTEN and ectopically expressed PTEN were clearly noted in the nuclei using this method (Fig. 1*B*). Control blots with antibodies against nuclear proteins RB and E2F family proteins confirmed the presence of these nuclear proteins in the nuclear extract and showed little or no cross-contamination of proteins in the cytosolic fraction (data not shown). Cytosolic contamination of the nuclear extracts prepared using the high salt technique (see "Materials and Methods") was also determined by assessing the LDH activity, a cytosolic marker, in nuclear and cytoplasmic fractions. Standard methods measuring decreasing absorbance at 340 nm showed that nuclear extracts exhibited LDH activity at or near background levels, whereas cytoplasmic samples showed typical high levels of activity (data not shown). The results from all control experiments indicated that little cytoplasmic contamination existed in the nuclear samples and that nuclear proteins were present in the nuclear fractions.

To determine whether the subcellular compartmentalization of PTEN was related to the cell cycle, this relationship was analyzed throughout the course of a cell cycle (approximately 24 h) using biochemical and flow cytometric approaches (Figs. 2 and 3) as well as by direct visualization (Fig. 4). The MCF-7 cells were synchronized with HU, which halts the cells in G_0-G_1, and subsequently released and harvested at the time points described above (see "Materials and Methods"). Cell cycle analysis was performed by flow cytometry using propidium iodide (Fig. 2). As shown in Fig. 2, using the same concentration of HU, the three cell lines all cycled with similar kinetics. On average, 70% of the cells were in G_0-G_1 at the time of

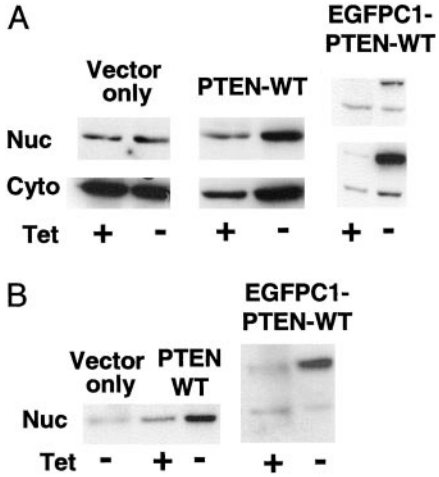

Fig. 1. Identification of nuclear (*Nuc*) and cytoplasmic (*Cyto*) PTEN in stably transfected MCF-7 Tet-off cell lines by Western blot using a monoclonal antibody to PTEN (6H2.1). *A*, stably transfected cell lines include vector only (pTre2Hyg), PTEN-WT (pTre2Hyg PTEN-WT), and EGFPC1-PTEN-WT (pTre2Hyg EGFPC1-PTEN-WT). Nuclear and cytoplasmic extracts were separated after withdrawal from Tet for 48 h (*Tet*−) using the high salt method (see "Materials and Methods"). The overexpression of PTEN-WT and EGFPC1-PTEN-WT was controlled with 2 μg/ml Tet (*Tet*+). In the EGFPC1-PTEN-WT line, the *bottom band* represents endogenous PTEN, and the *top band* represents the transfected EGFPC1-PTEN fusion product. *B*, confirmation of nuclear PTEN using a sucrose gradient method of nuclear extract preparation. The overexpression of PTEN-WT and EGFPC1-PTEN-WT was controlled with 2 μg/ml Tet. In the EGFPC1-PTEN-WT cell line, the *bottom band* represents endogenous PTEN, and the *top band* represents the transfected EGFPC1-PTEN fusion product.

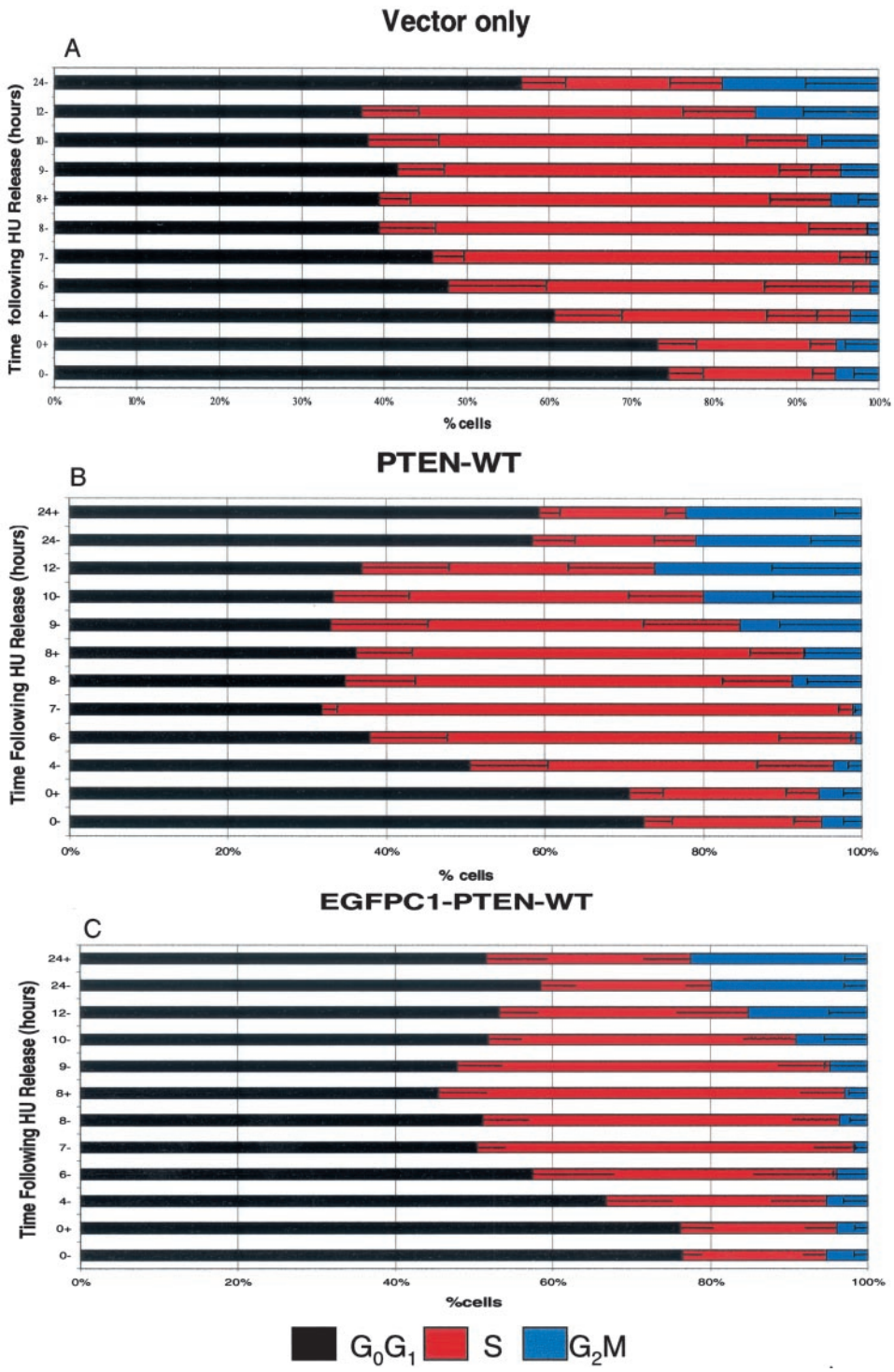

Fig. 2. Relationship of nuclear and cytoplasmic PTEN during the cell cycle in MCF-7 cell lines. *A*, vector only (pTre2Hyg). Peak G_0-G_1 fraction occurred at 0, 4, and 24 h after HU release; the highest S-phase percentage occurred at 7–8 h. *B*, PTEN-WT (pTre2Hyg PTEN-WT). Peak G_0-G_1 fraction occurred at 0 and 24 h after HU release; the highest S-phase percentage occurred at 6–7 h. *C*, EGFPC1-PTEN-WT (pTre2Hyg EGFPC1-PTEN-WT). Peak G_0-G_1 fractions occurred at 0, 4, and 24 h after HU release; the highest S-phase percentage occurred at 7–8 h.

HU release, reached S phase by 6–9 h, and returned to 60% G_0-G_1 by 24 h. The similarity of cell cycle timing allowed the comparison of the cycled EGFPC1-PTEN-WT grown on slides with Western blots from all three cell lines. Cytoplasmic and nuclear extracts from time points throughout a cell cycle were then subjected to Western blot analysis for PTEN (Fig. 3). Ponceau S staining confirmed equal protein loading (Fig. 3*A*). All three cell lines had nuclear and cytoplasmic PTEN, the levels of which clearly varied with the cell cycle (Fig. 3, *A–C*). In the case of the EGFPC1-PTEN-WT, both EGFPC1-PTEN (*top band*) and endogenous PTEN (*bottom band*) can be noted on the Western blots (Fig. 3*C*). Differential levels of nuclear and cytoplasmic PTEN were associated with changes in the percentages of cells in a given phase at the time of harvest. In general, the highest levels of nuclear, as well as cytosolic, PTEN were associated with the greatest proportion of cells in G_0-G_1 at the 0, 4, and 24 h time points (Figs. 2 and 3). Note that nuclear (and cytoplasmic) PTEN levels began to increase at the 12 h time point as the cells begin to leave G_2-M and enter G_1 (Fig. 3). Overexpression of PTEN in this cell line has been shown by our laboratory and others to induce G_1 arrest (11–13). Therefore, in addition to PTEN's cytosolic signaling leading to G_1 arrest, our observations of increased nuclear PTEN at and around G_0-G_1 may suggest that PTEN can also act in the nucleus to effect G_1 blockade.

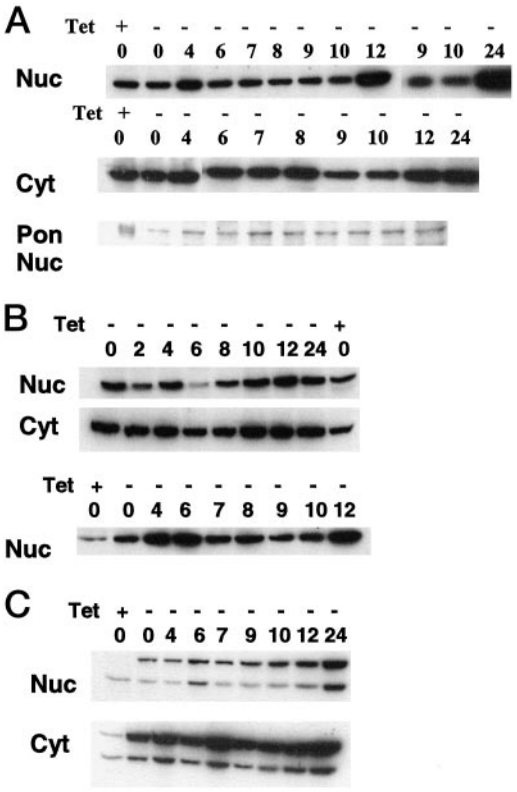

Fig. 3. PTEN in nuclear (*Nuc*) and cytoplasmic (*Cyt*) extracts from MCF-7-transfected cells after cell synchronization in G_0-G_1 and release. Cells were released and harvested at time points over a 24 h peroid. Equal loading was confirmed with Ponceau S staining (*Pon Nuc*). These blots are representative of at least five time course experiments for each cell line and do not show all time points collected or tested. *A*, vector only (pTre2Hyg). Nuclear PTEN protein levels were increased at the 0, 4, 12, and 24 h time points. *B*, PTEN-WT (pTre2Hyg PTEN-WT) levels in the nuclei were increased at the 0, 4, 12, and 24 h time points. An additional nuclear time course is shown to demonstrate similarity of results. *C*, EGFPC1-PTEN-WT (pTre2Hyg EGFPC1-PTEN-WT) nuclear concentrations were increased at the 0, 4, 12, and 24 h time points.

Although a G_1 block was not observed here in the cell lines overexpressing PTEN, cells in this series were synchronized in contrast to previously published studies with freely cycling cells. Normal cells proliferate in the presence of PTEN, and therefore PTEN alone does not control cell cycle progression (15). Lower PTEN levels were associated with an increase in cells in the S phase for all cell lines, although the precise time point varied slightly both with individual experiments and with the construct. However, the overexpression of neither PTEN-WT nor EGFPC1-PTEN-WT appeared to affect the kinetics of the cell cycle or the entry of PTEN into the nucleus.

The biochemical data demonstrating differential levels of nuclear and cytoplasmic PTEN with the cell cycle were corroborated by those noted by directly visualizing EGFPC1-PTEN-WT in slide well-grown MCF-7 cells (Fig. 4*A*). PTEN expression was visualized as GFP expression, *i.e.*, green fluorescence; nuclei were marked with blue DNA stain (Hoechst 33342); and thus, the overlap could be delineated. As with the biochemical observations above, both nuclear and cytoplasmic PTEN protein levels changed with the cell cycle (Fig. 3). Although PTEN was still apparent in the nucleus at the 8, 9, and 10 h time points after HU release, a markedly decreased intensity was observed in the majority of cells (Fig. 4*A*). The highest levels of nuclear EGFPC1-PTEN were seen at the 0 and 24 h time points, followed by that at the 12 h time point. The changes in nuclear PTEN can be further appreciated in the overlap panels of Fig. 4, where the overlap of green nuclear PTEN and dark blue DNA stain appears as a light blue-green that is particularly intense at the 0, 12, and 24 h time

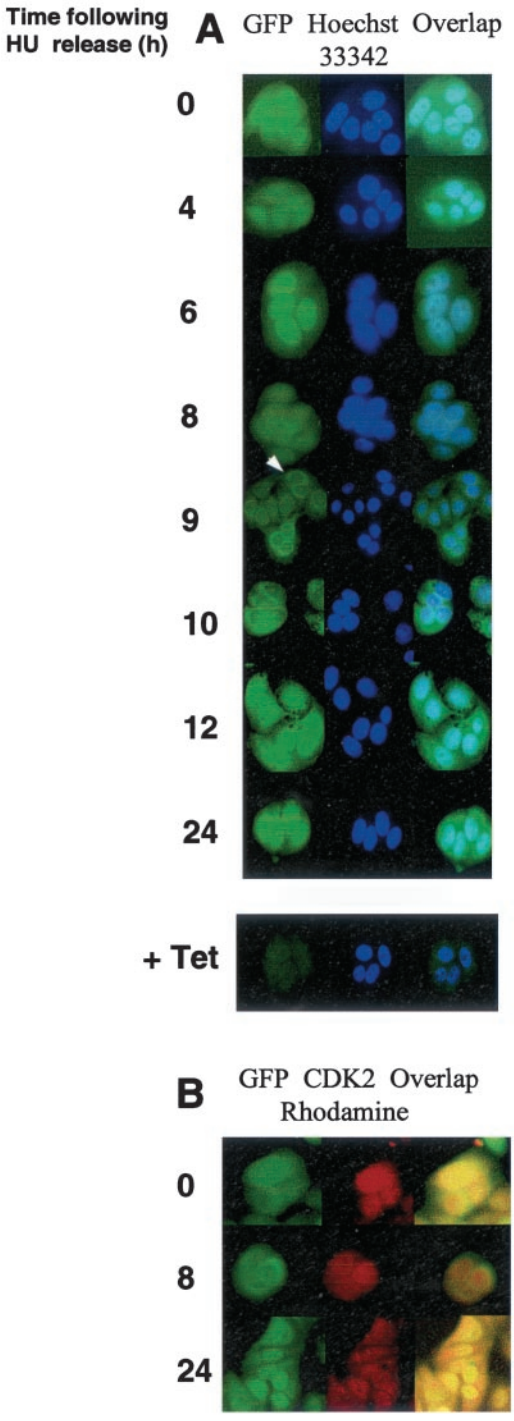

Fig. 4. Localization of EGFPC1-PTEN-WT in MCF-7 cells harvested at time points after release from the cell cycle. *A*, colocalization of EGFPC1-PTEN-WT with Hoechst 33342. *Left*, EGFPC1-PTEN expression is represented in *green*. *Middle*, Hoechst 33342 filtered for DNA staining is represented in *dark blue*. *Right*, the overlap of images from the *left* and *middle* where *light blue-green* represents the overlap of *green* EGFPC1-PTEN and *blue* DNA staining, whereas the *dark blue* represents DNA staining alone. Each image is representative of a minimum three sets of slides for each time point. Note should be made of the most intense GFP staining at the 0, 12, and 24 h time points, with the least intense staining observed at the 8, 9, and 10 h time points. The *closed white arrow* (9 h time point) indicates potential accumulation of EGFPC1-PTEN at the outer face of the nuclear membrane in some cells. Tet abrogated EGFPC1-PTEN-WT expression (+*Tet*) in the *bottom row* of images. *B*, EGFPC1-PTEN colocalization with CDK2, a nuclear protein. *Left*, EGFPC1-PTEN is represented in *green*. *Middle*, rhodamine-tagged CDK2 is represented in *red*. *Right*, the overlap of EGFPC1-PTEN and CDK2 is represented in *yellow*. Only the 0, 8, and 24 time points are shown as representative of panels similar to those shown in *A*. Nuclear PTEN was highest at the 0 and 24 h time points and lowest at the 8 h time point after release from HU.

points, where nuclear PTEN levels peak. The dark blue DNA-only stain is more evident in the 8, 9, and 10 h time points, where nuclear PTEN levels are at the nadir (Fig. 4*A*). Interestingly, at the 8–10 h time points, when nuclear PTEN is at its lowest point, an increased concentration of PTEN can be seen as a halo around or at the nuclear membrane (Fig. 4*A*). This may represent an area of increased cytoplasmic density, as suggested by other researchers (16) examining PTEN in fibroblasts; whether PTEN accumulates at the nuclear membrane merits further investigation. A recent study of protein-protein interactions showed that PTEN, through its C2 domain, could bind the MVP (17). Some members of the vault family bind proteins near the nuclear membrane, enabling them to become adjacent to the nuclear pore. PTEN could use MVP to cross the nuclear membrane. These observations with Hoechst 33342 nuclear stain were correlated with a second series of studies in which cells were incubated with antibodies to CDK2, a nuclear protein, and a secondary antibody tagged with rhodamine to visualize the CDK2. The results of the time course after release from HU were similar to those of samples with EGFPC1-PTEN and Hoechst staining alone. Higher levels of nuclear PTEN occurred at time points corresponding to G_0-G_1, and less nuclear PTEN was found when cells were in S phase. Again, EGFPC1-PTEN is shown as *green* in the first column, CDK2 is shown as *red* in the second column, and the overlap could be clearly observed as *yello*w in the third column (Fig. 4*B*). Time points examined were the same as those shown with the Hoechst stain only in Fig. 4*A*, but only the 0, 8, and 24 h time points are shown as representative of the time course (Fig. 4*B*). Nuclear PTEN again appears to be most prominent in the 0 and 24 h time points when cells are in G_1 as shown by the *yellow* overlap of CDK2 and EGFPC1-PTEN in the nucleus. Decreased nuclear PTEN, as shown by the *red* stain only in the nucleus, in the 8 h post-HU release sample occurred when cells were primarily in S phase.

Through the use of fluorescent antibodies and other techniques, PTEN has been shown in the cytoplasm in MCF-7 (11); U87, U178, and LN229 (18); and 293T (19) cancer cell lines. Our current observation is the first to directly demonstrate the presence of nuclear PTEN in MCF-7 breast cancer cells. PTEN does not have a traditional NLS; therefore, previous immunohistochemical and anecdotal observations of PTEN in the nucleus may be artifacts of experimentation. However, we have now directly demonstrated, using biochemical and cell biological strategies, that PTEN can exist in the nucleus of the MCF-7 breast cancer cell line. Although localization mechanisms typically require a NLS and accessory proteins to negotiate the nuclear pore complex, PTEN may have an alternatively structured sequence. The traditional NLS is a repeat of positive aa with flanking proline, but proteins may have a less traditionally structured region termed a nuclear-cytoplasmic shuttling sequence or a bipartite NLS sequence (20). PTEN may have one of these less typical NLSs. Also, the postsynaptic density protein/*Drosophila* disc large/zona occludens-1 domain or other areas, such as that shown with the C2 domain interaction with MVP, may offer mechanisms for the binding of PTEN to a partner protein for nuclear import. Furthermore, naturally occurring germ-line or somatic mutations displaying altered nuclear PTEN may offer insight into areas that promote nuclear entry or export. Our unambiguous demonstration of PTEN in the nucleus makes identification of either a nontraditional NLS or partnering proteins with a NLS a feasible target for further exploration. In addition, because we observe peak nuclear PTEN levels at or before G_0-G_1 and nadir at S phase, we postulate that PTEN may also play a role in the nucleus to help coordinate, at the least, cell cycle arrest. Because total sequestration from the cytoplasm was not observed in these studies, PTEN therefore still functions in this compartment. A new role for PTEN in the nucleus and the relationship of nuclear PTEN to cell cycle-related proteins should also be examined.

Acknowledgments

We thank Dr. K. A. Waite, Dr. S. Tanner, Dr. C. Timmers, Dr. G. Leone, Dr. D. Guttridge, and J. Austin for helpful discussions and for assistance with the design of plasmid constructs. We also thank Dr. H. Saavarda for aid with fluorescent microscopy and A. Oberyszyn for cell cycle data analysis.

References

1. Li, J., Yen, C., Liaw, D., Podsypanina, K., Bose, S., Wang, S. I., Puc, J., Miliaresis, C., Rodgers, L., McCombie, R., Bigner, S. H., Giovanella, B. C., Ittmann, M., Tycko, B., Hibshoosh, H., Wigler, M. H., and Parsons, R. PTEN, a putative protein tyrosine phosphatase gene mutated in human brain, breast, and prostate cancer. Science (Wash. DC), *275:* 1943–1947, 1997.
2. Steck, P. A., Pershouse, M. A., Jasser, S. A., Yung, W. K., Lin, H., Ligon, A. H., Langford, L. A., Baumgard, M. L., Hattier, T., Davis, T., Frye, C., Hu, R., Swedlund, B., Teng, D. H., and Tavtigian, S. V. Identification of a candidate tumour suppressor gene, MMAC1, at chromosome 10q23.3 that is mutated in multiple advanced cancers. Nat. Genet., *15:* 356–362, 1997.
3. Vazquez, F., and Sellers, W. R. The PTEN tumor suppressor protein: an antagonist of phosphoinositide 3-kinase signaling. Biochim. Biophys. Acta, *1470:* M21–M35, 2000.
4. Gimm, O., Perren, A., Weng, L. P., Marsh, D. J., Yeh, J. J., Ziebold, U., Gil, E., Hinze, R., Delbridge, L., Lees, J. A., Mutter, G. L., Robinson, B. G., Komminoth, P., Dralle, H., and Eng, C. Differential nuclear and cytoplasmic expression of PTEN in normal thyroid tissue and benign and malignant epithelial thyroid tumors. Am. J. Pathol., *156:* 1693–1700, 2000.
5. Perren, A., Komminoth, P., Saremaslani, P., Matter, C., Feurer, S., Lees, J. A., Heitz, P. U., and Eng, C. Mutation and expression analyses reveal differential subcellular compartmentalization of PTEN in endocrine pancreatic tumors compared to normal islet cells. Am. J. Pathol., *157:* 1097–1103, 2000.
6. Whiteman, D. C., Zhou, X. P., Cummings, M. C., Pavey, S., Hayward, N. K., and Eng, C. Nuclear PTEN expression and clinicopathologic features in a population-based series of primary cutaneous melanoma. Int. J. Cancer, *99:* 63–67, 2002.
7. Tachibana, M., Shibakita, M., Ohno, S., Kinugasa, S., Yoshimura, H., Ueda, S., Fujii, T., Rahman, M. A., Dhar, D. K., and Nagasue, N. Expression and prognostic significance of PTEN product protein in patients with esophageal squamous cell carcinoma. Cancer (Phila.), *94:* 1955–1960, 2002.
8. Zhou, X. P., Kuismanen, S., Nystrom-Lahti, M., Peltomaki, P., and Eng, C. Distinct PTEN mutational spectra in hereditary non-polyposis colon cancer syndrome-related endometrial carcinomas compared to sporadic microsatellite unstable tumors. Hum. Mol. Genet., *11:* 445–450, 2002.
9. Lachyankar, M. B., Sultana, N., Schonhoff, C. M., Mitra, P., Poluha, W., Lambert, S., Quesenberry, P. J., Litofsky, N. S., Recht, L. D., Nabi, R., Miller, S. J., Ohta, S., Neel, B. G., and Ross, A. H. A role for nuclear PTEN in neuronal differentiation. J. Neurosci., *20:* 1404–1413, 2000.
10. Li, L., Ernsting, B. R., Wishart, M. J., Lohse, D. L., and Dixon, J. E. A family of putative tumor suppressors is structurally and functionally conserved in humans and yeast. J. Biol. Chem., *272:* 29403–29406, 1997.
11. Hlobilkova, A., Guldberg, P., Thullberg, M., Zeuthen, J., Lukas, J., and Bartek, J. Cell cycle arrest by the PTEN tumor suppressor is target cell specific and may require protein phosphatase activity. Exp. Cell Res., *256:* 571–577, 2000.
12. Weng, L. P., Smith, W. M., Dahia, P. L., Ziebold, U., Gil, E., Lees, J. A., and Eng, C. PTEN suppresses breast cancer cell growth by phosphatase activity-dependent G_1 arrest followed by cell death. Cancer Res., *59:* 5808–5814, 1999.
13. Zhu, X., Kwon, C. H., Schlosshauer, P. W., Ellenson, L. H., and Baker, S. J. PTEN induces G_1 cell cycle arrest and decreases cyclin D3 levels in endometrial carcinoma cells. Cancer Res., *61:* 4569–4575, 2001.
14. Davezac, N., Baldin, V., Gabrielli, B., Forrest, A., Theis-Febvre, N., Yashida, M., and Ducommun, B. Regulation of CDC25B phosphatases subcellular localization. Oncogene, *19:* 2179–2185, 2000.
15. Yamada, K. M., and Araki, M. Tumor suppressor PTEN: modulator of cell signaling, growth, migration and apoptosis. J. Cell Sci., *114:* 2375–2382, 2001.
16. Tamura, M., Gu, J., Matsumoto, K., Aota, S., Parsons, R., and Yamada, K. M. Inhibition of cell migration, spreading, and focal adhesions by tumor suppressor PTEN. Science (Wash. DC), *280:* 1614–1617, 1998.
17. Yu, Z., Fotouhi-Aroakani, N., Wu, L., Maoui, M., Wang, S., Banville, D., and Shen, S. H. PTEN associates with the vault particles in HeLa cells. J. Biol. Chem., *277:* 40247–40252, 2002.
18. Furnari, F. B., Lin, H., Huang, H. S., and Cavenee, W. K. Growth suppression of glioma cells by PTEN requires a functional phosphatase catalytic domain. Proc. Natl. Acad. Sci. USA, *94:* 12479–12484, 1997.
19. Mayo, L. D., Dixon, J. E., Durden, D. L., Tonks, N. K., and Donner, D. B. PTEN protects p53 from Mdm2 and sensitizes cancer cells to chemotherapy. J. Biol. Chem., *277:* 5484–5489, 2002.
20. Liang, S. H., and Clarke, M. F. A bipartite nuclear localization signal is required for p53 nuclear import regulated by a carboxyl-terminal domain. J. Biol. Chem., *274:* 32699–32703, 1999.